Surface Science 125 (1983) 429–451
North-Holland Publishing Company

SPECIFIC ADSORPTION OF HALIDE AND PSEUDOHALIDE IONS AT ELECTROCHEMICALLY ROUGHENED VERSUS SMOOTH SILVER–AQUEOUS INTERFACES

Joseph T. HUPP, D. LARKIN * and Michael J. WEAVER **

Department of Chemistry, Purdue University, West Lafayette, Indiana 47907, USA

Received 13 September 1982; accepted for publication 16 November 1982

The differential capacitance of electrochemically roughened silver surfaces in mixed perchlorate electrolytes containing chloride, bromide, iodide, thiocyanate, or azide anions has been measured as a function of electrode potential and anion concentration. These results are compared with corresponding data for electropolished silver in order to ascertain the influence of surface roughening on the double-layer structure and composition of polycrystalline silver–aqueous interfaces. The surface concentrations of specifically adsorbed anions were obtained from these capacitance–potential data using a "Hurwitz–Parsons" type of analysis. Although electrochemical roughening by means of a conventional oxidation–reduction cycle in chloride media is a prerequisite to the appearance of Surface-Enhanced Raman Scattering (SERS) for these adsorbates, it yields only moderate (ca. 1.5- to 2-fold) increases in the actual surface area and has a relatively minor effect on their average surface concentration. However, roughening does induce noticeable changes in the morphology of the capacitance–potential curves which are traced to alterations in the surface-crystallite structure. Comparisons between the potential dependence of SERS with corresponding capacitance–potential data indicate that anion coverages close to a monolayer are necessary for stable SERS. This is attributed to the stabilization of Raman-active silver clusters by surrounding adsorbed anions.

1. Introduction

The discovery of Surface-Enhanced Raman Scattering (SERS) from adsorbates at silver electrodes that have been roughened by means of a prior "oxidation–reduction cycle" (ORC) [1] has generated intense interest in characterizing the nature of the physical phenomena involved. The effect shows promise of providing a valuable in situ spectroscopic tool for elucidating the microscopic structure of metal–electrolyte interfaces. A central question to be addressed for this purpose is the relationship between the nature and intensity

* Permanent address: Department of Chemistry, Towson State University, Towson, Maryland 21204, USA.
** To whom correspondence should be addressed.

0039-6028/83/0000–0000/$03.00

of the SERS signals and the structure and composition of the metal–electrolyte interfaces, especially the surface concentration of the adsorbate acting as the Raman scatterer. However, little progress on this matter has been made to date; the required studies of the interfacial composition under conditions where SERS are observed have largely been conspicuous by their absence.

Halide and pseudohalide anions form an especially interesting series of model adsorbates for fundamental SERS studies in view of their simple structure and tendency to adsorb strongly at a number of solid metals, including the silver–aqueous interface which has been utilized in most Raman investigations so far. Most importantly, the anionic surface concentrations can be determined quantitatively from measurements of the differential double-layer capacitance C_d against the electrode potential E for varying bulk concentrations of the adsorbing anions [2,3], using the so-called "Hurwitz–Parsons" analysis [4]. Silver is an especially tractable metal for this purpose since surprisingly reproducible values of C_d that are largely independent of the applied a.c. frequency can be obtained at smooth electropolished surfaces [2,3,5]. Nevertheless, this simple yet powerful method for extracting the surface compositional data needed for the quantitative interpretation of SERS has received scant attention by practitioners in this area.

We have recently obtained specific adsorption data for chloride, bromide, iodide, azide, and thiocyanate at a polycrystalline silver–aqueous interface from C_d–E data and also using a "kinetic probe" technique [3]. Although these anions are very strongly adsorbed, especially at more positive potentials, these surfaces exhibit no detectable Raman scattering. However, mild ORC roughening, corresponding to the redeposition of only a few silver layers, can yield surfaces displaying measurable Raman scattering for these and other inorganic adsorbates [6,7]. It is therefore of interest to explore the influence of electrochemical roughening on the double-layer structure of the silver–aqueous interface, in particular on the surface concentration of such structurally simple adsorbates. Fleischmann et al. have recently noted the effect of severe electrochemical roughening upon the capacitance of a silver electrode in chloride media, although no thermodynamic analysis of the data was undertaken [8].

We report here specific adsorption measurements for chloride, bromide, iodide, azide, and thiocyanate obtained from C_d–E data at electrochemically roughened silver electrodes. These are compared with corresponding data gathered at a smooth polycrystalline surface. The results indicate that the surface roughening procedure that is crucial to SERS has a relatively small influence on the average surface concentration of these anions, although noticeable changes occur in the morphology of the capacitance–potential curves. The data enable quantitative comparisons to be made between the appearance of SERS and the average surface concentration of the Raman scatterers.

2. Experimental

Experimental details were mostly as described in ref. [3], including the preparation of smooth silver surfaces using a cyanide electropolishing technique. The silver electrode was fabricated as a silver rod sheathed in Teflon. It was electrochemically roughened using the following procedure. After mechanical polishing using 1.0 and then 0.3 μm alumina on a polishing wheel, the electrode was immersed in 0.1M KCl at -140 mV versus a saturated calomel electrode (SCE). The electrode was then subjected to an ORC of the same type employed in SERS studies [7] by stepping the potential to 210 mV and held there until a known quantity of anodic charge q_{ORC} had been passed, typically 20–40 mC cm^{-2}. The potential was then returned to and held at -140 mV until an essentially equal amount of cathodic charge had been passed. The electrode was then soaked in 2M $HClO_4$ for 15 min in order to remove residual adsorbed chloride.

The capacitance was measured using a phase sensitive detection method [3]. Simultaneous recordings of in-phase and quadrature components were made using a lock-in amplifier with an internal oscillator usually set at a frequency of 100 Hz and 4 mV peak-to-peak AC amplitude. Both in-phase and quadrature components were taken into account in calculating C_d [3]. Values of C_d as a function of electrode potential were obtained by sweeping the potential, usually at 2–5 mV s^{-1}, using a PAR 175 potential programmer together with a PAR 173 potentiostat. Under these conditions, essentially identical C_d–E curves were obtained irrespective of the direction of the potential scan.

All measurements were made at room temperature, 23 ± 0.5°C. Electrode potentials were measured with respect to a saturated calomel electrode filled with NaCl rather than KCl in order to avoid precipitation of $KClO_4$ in the liquid junction, but all are reported here with respect to the conventional SCE.

3. Results and discussion

3.1. Determination of roughness factors for silver surfaces

Fig. 1 shows three representative C_d–E curves obtained for polycrystalline silver in contact with 0.5M $NaClO_4$. This medium was chosen as the "inert" background electrolyte for the present studies in view of the relatively weak adsorption of perchlorate. Although we previously used 0.5M NaF for this purpose [3], fluoride anions appear to be more strongly adsorbed than perchlorate on silver [9], so that 0.5M $NaClO_4$ is preferred here. The lowest curve in fig. 1 was obtained after electropolishing the electrode in a cyanide medium [3], whereas the upper two curves were measured following oxidation–reduction cycles in 0.1M KCl as described above. Both these ORCs involved passing

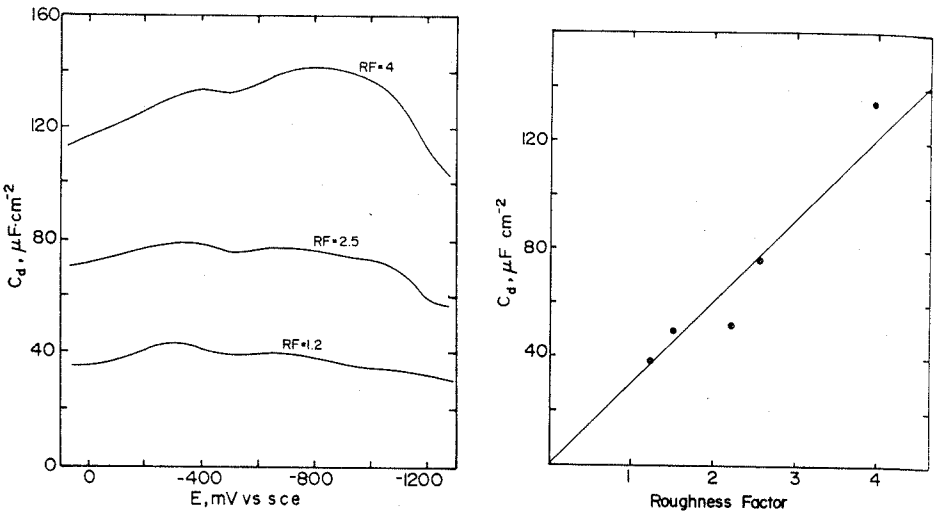

Fig. 1. Differential capacitance of polycrystalline silver in 0.5M $NaClO_4$ plotted against electrode potential for various roughness factors (RF) indicated.

Fig. 2. Differential capacitance for polycrystalline silver at -550 mV versus roughness factor as determined using lead upd method (see text).

greater amounts of anodic charge (ca. 50 and 120 mC cm^{-2} for the middle and upper curves, respectively), than are normally required in order to induce SERS for adsorbed anions such as chloride. Nevertheless, no marked changes in the shape of the C_d–E curves are seen, the capacitance increasing monotonically with increasing roughness brought about by passing larger quantities of anodic charge, q_{ORC}, during the ORC. This suggests that approximate estimates of the roughness factor RF (i.e., the ratio of the actual to geometric surface area) can be obtained simply from the ratio of measured capacitances at a given electrode potential with respect to that for a smooth surface.

This method for determining RF was checked against an alternative approach which involved measuring the faradaic charge consumed for the deposition or redissolution of a monolayer of underpotential deposited (UPD) lead [10–12]. The procedure entailed measuring the charge under the cathodic–anodic cyclic voltammetric peaks obtained in the potential region -300 to -400 mV for a solution containing 5 mM Pb^{2+}. Essentially symmetrical cyclic voltammograms were obtained using slow sweep rates (ca. 5 mV s^{-1}) which also minimized the contribution of double-layer charging. The roughness factor was calculated by assuming that the charge required for deposition (or redissolution) of a monolayer of lead atoms on a perfectly smooth silver surface equals 310 μC cm^{-2} [10]. Three voltammetric peaks

could be resolved, at about −300, −320, and −350 mV. Roughening the electrode produced little change in the appearance of the cyclic voltammograms besides enhancing the current. This together with the similar form of the C_d–E curves seen in fig. 1, indicates that no major changes are occurring in the average microscopic properties of the silver surface beyond an increase in the overall surface area.

Generally, the values of RF obtained from the double-layer capacitances agree quite well (within ca. 10–20%) with those found using the lead UPD method (fig. 2). Electrodes roughened sufficiently to yield intense SERS signals, say $q_{ORC} > 10$ mC cm^{-2}, exhibited only moderate roughness factors; thus typically RF ~ 1.5–2 for $q_{ORC} = 20$ mC cm^{-2}. For electropolished silver it was found that RF ≈ 1.2 from the lead UPD method. The values of RF for the roughened electrodes were somewhat irreproducible, depending upon the exact manner of the washing and soaking steps following the ORC. An examination of these factors was made by recording C_d–E curves in the 0.1M KCl electrolyte used for the ORC. A C_d–E curve obtained immediately after an ORC by scanning the potential from −100 mV to and from various more negative potentials out to −1200 mV exhibited negligible hysteresis even after several potential scans over a period of 15–20 min. Interestingly, this reversibility is in complete contrast to the behavior of the SERS 240 cm^{-1} mode (silver–chloride stretching) for adsorbed chloride which is almost entirely and irreversibly quenched upon scanning more negative than ca. −500 mV under these conditions [13]. Washing and soaking the roughened electrode in perchloric acid yielded significant decreases in the capacitance in 0.1M KCl, corresponding to RF decreases of up to ca. 30%, depending on the vigor of the washing procedure and the soaking time (up to ca. 30 min). Nevertheless, the individual C_d–E curves obtained after returning the electrode to the cell consistently exhibited little or no hysteresis.

Although most capacitance data were obtained using an AC frequency of 100 Hz, the frequency dependence of C_d was also examined. Over the frequency range 20–1500 Hz in 0.5M $NaClO_4$, the apparent values of C_d generally increased with decreasing frequency, although only of the order of ca. 10% for every 10-fold frequency change. The extent of this frequency dispersion was similar on roughened and electropolished surfaces, and largely independent of the electrode potential. This behavior is somewhat more ideal than found for electropolished silver in 0.5M NaF, where noticeably greater frequency dispersions were found at potentials positive of ca. −700 mV [3].

3.2. Determination of anion specific adsorption

These results indicate that the electrochemically roughened silver surfaces exhibit sufficiently well-behaved and reproducible behavior to allow quantitative estimates of specific anion adsorption to be obtained from C_d–E data

using the Hurwitz–Parsons approach. Following our earlier measurements [3], C_d–E curves were recorded in a series of mixed electrolytes having the general composition $(0.5 - x)$M $NaClO_4 + x$M NaX, where X is the adsorbing anion, either Cl^-, Br^-, I^-, NCS^-, or N_3^-. The general procedure was to record a C_d–E curve for a previously roughened or electropolished silver electrode in 0.5M $NaClO_4$, and then obtain C_d–E curves following successive additions of NaX using the same electrode.

The surface concentrations of specifically adsorbed anions were calculated from each family of C_d–E curves using two variants of the Hurwitz–Parsons analysis, as follows. The Gibbs adsorption equation for the mixed electrolytes employed here can be written as [4b]

$$-\mathrm{d}\gamma = q^m \,\mathrm{d}E + \{\Gamma_X - [x/(0.5 - x)]\,\Gamma_{ClO_4}\}RT\,\mathrm{d}\ln x, \tag{1}$$

where γ is the surface tension, q^m is the excess electronic charge density on the metal surface, E is the electrode potential, and Γ_X and Γ_{ClO_4} are the surface excesses of the added anion X and the perchlorate anion. Provided that the components of Γ_X and Γ_{ClO_4} in the diffuse layer, Γ_X^d and $\Gamma_{ClO_4}^d$ respectively, are present in the same ratio as the anion mole fractions, i.e. $\Gamma_X^d/\Gamma_{ClO_4}^d = x/(0.5 - x)$, as expected [4b], then eq. (1) can be rewritten as

$$-\mathrm{d}\gamma = q^m \,\mathrm{d}E + \{\Gamma'_X - [x/(0.5 - x)]\,\Gamma'_{ClO_4}\}RT\,\mathrm{d}\ln x, \tag{2}$$

where Γ'_X and Γ'_{ClO_4} are the components of Γ_X and Γ_{ClO_4} present in the inner layer, i.e. the surface concentrations of specifically adsorbed anions. Providing Γ'_{ClO_4} is small (vide supra), we can write

$$-\mathrm{d}\gamma = q^m \,\mathrm{d}E - \Gamma'_X RT\,\mathrm{d}\ln x. \tag{3}$$

Eq. (3) suggests that the desired values of Γ'_X can be obtained simply from

$$\Gamma'_X = -(1/RT)(\partial\gamma/\partial \ln x)_E. \tag{4}$$

The required coefficients $(\partial\gamma/\partial \ln x)_E$ were obtained from the C_d–E curves by noting that the observed coincidence of these curves at negative potentials will also be associated with values of q^m and γ that are both independent of x. Therefore the C_d–E curves can be double integrated to yield a corresponding set of $\Delta\gamma$–E curves, where $\Delta\gamma$ is the surface tension with respect to the (unknown) value at some suitably negative potential. (Since the C_d–E curves were often not quite coincident at the most negative potentials (ca. -1300 to -1400 mV) at which C_d could be accurately evaluated due to the onset of hydrogen evolution, a short extrapolation of these curves to more negative potentials was required.) The required values of $(\partial\gamma/\partial \ln x)_E$ were obtained for various values of x and E from the family of $\Delta\gamma$–E curves, yielding plots of Γ'_X against E for various values of x. We shall denote this approach as Method I. It has been recently employed, for example, to determine chloride specific adsorption at single-crystal silver surfaces [2].

We have previously used a related approach, denoted here as Method II [3,14,15], based on the following "cross-differential" relation which can be obtained from eq. (1) [14]:

$$(\partial q^m/\partial \Gamma'_X)_E = -RT(\partial \ln x/\partial E)_{\Gamma'_X}. \quad (5)$$

Provided that the coefficient $(\partial q^m/\partial \Gamma'_X)_E$ is essentially independent of coverage, Γ'_X can be found from

$$\Gamma'_X = -(\Delta q^m)_E/RT(\partial \ln x/\partial E)_{\Gamma'_X}, \quad (6)$$

where $(\Delta q^m)_E$ is the change in electrode charge density at a given electrode potential brought about by the addition of the adsorbing anion X. This quantity can easily be found by back-integrating the C_d–E curves as before, but only once to yield a family of relative q^m–E curves. The required coefficient $(\partial \ln x/\partial E)_{\Gamma'_X}$ can be evaluated from the relative shape of these q^m–E curves as described in ref. [14]. [Note that Methods I and II require only information on the *changes* in q^m (or $\Delta\gamma$) brought about by altering the anion concentration, x, so that a knowledge of the potential of zero charge or absolute values of q^m is not required.]

Although Method II provides a particularly direct route to Γ'_X, it is desirable that the coefficients in eq. (3) be essentially independent of anion surface concentration and electrode potential. For the present systems, $-(\partial \ln x/\partial E)_{\Gamma'_X}$ (or the closely related dimensionless quantity $-(RT/F)(\partial \ln x/\partial E)_{\Gamma'_X}$, the "electrosorption valency" EV) was found to depend not only on coverage but to decrease noticeably as the electrode potential becomes less negative, eventually even changing sign at the most positive potentials. Therefore Method I was chiefly employed in the present study, although Method II gave essentially the same results. The latter was found to be especially useful for extracting values of Γ'_X at extreme low and high anion concentrations.

Fig. 3a shows a typical set of C_d–E curves for electropolished silver (RF ≈ 1.2) in a series of mixed $NaClO_4$–NaCl electrolytes with $x = 0$ to 0.2M, and fig. 3b gives a corresponding set gathered for a roughened silver electrode ($q_{ORC} = 40$ mC cm^{-2}, RF = 1.9). Comparisons of figs. 3a and 3b show that the general features of the C_d–E curves are similar on the smooth and roughened electrodes (vide supra). The latter curves have values of C_d that are about 50% higher, in accordance with the measured roughness factor. (Here and elsewhere C_d is reported in terms of the geometrical (apparent) surface area.) At potentials more negative than ca. −1300 mV, the capacitance is almost independent of the bulk chloride concentration, indicating that here chloride specific adsorption is negligible. As the potential becomes less negative, progressive increases in C_d are seen for the chloride-containing solutions which become larger with increasing bulk concentration as a consequence of greater chloride specific adsorption.

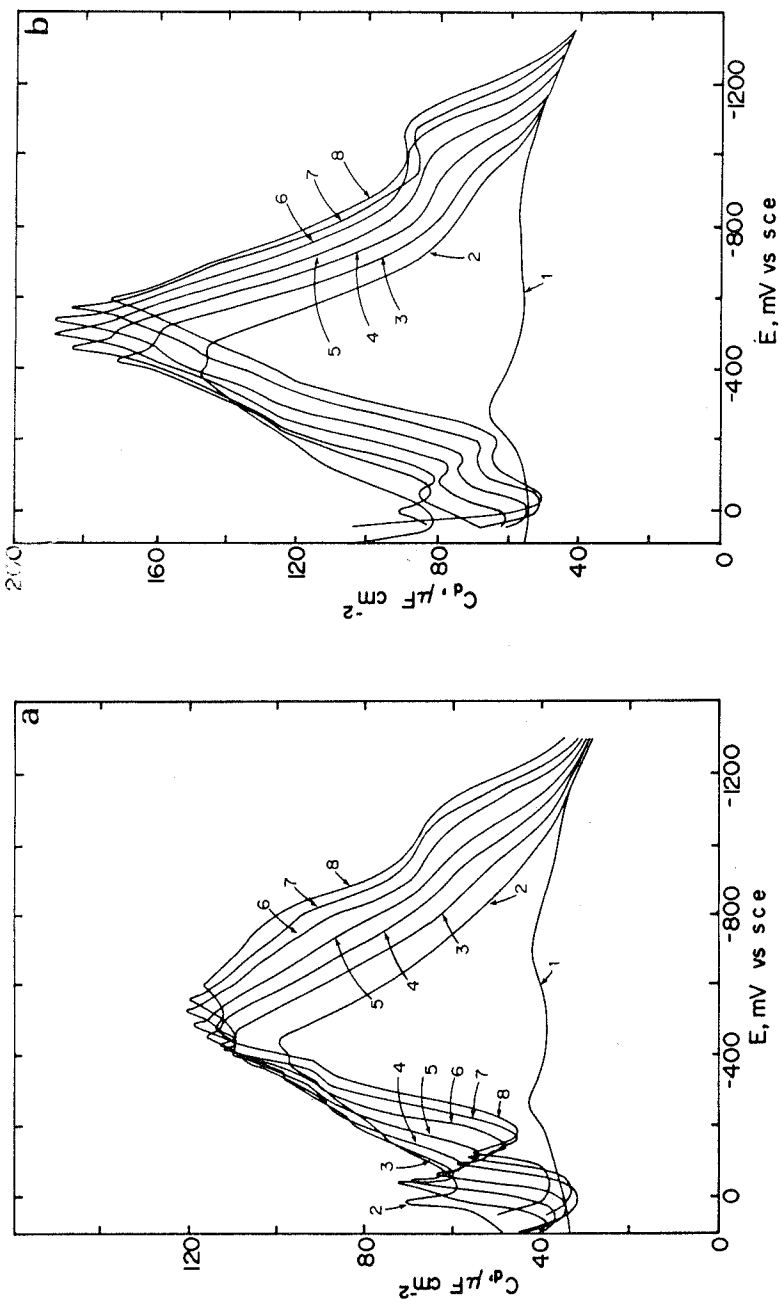

Fig. 3. (a) Differential capacitance versus electrode potential for electropolished polycrystalline silver (RF ≈ 1.2) in $NaClO_4$–NaCl mixtures at ionic strength 0.5. Key to chloride concentrations: (1) 0; (2) 1mM; (3) 2.5mM; (4) 6mM; (5) 15mM; (6) 40mM; (7) 100mM; (8) 200mM. (b) As in (a), but for electrochemically roughened silver (RF ≈ 1.9).

The resulting values of Γ'_{Cl} as a function of potential for two chloride concentrations, 0.015M and 0.1M, are shown in fig. 4 for both electropolished (solid curves) and roughened surfaces (dashed curves). (The surface concentrations here and below are reported in terms of the *actual* surface area, i.e. by taking into account the measured roughness factors RF ≈ 1.2 and 1.9 for the electropolished and roughened surfaces, respectively.) It is seen that the corresponding Γ'_{Cl} values are somewhat *smaller* on the roughened compared to the electropolished surface, and only increase marginally with increasing bulk chloride concentration. Although the decrease in Γ'_{Cl} upon surface roughening is relatively mild (up to ca. 30%) it is considered to be greater than the experimental uncertainty in Γ'_X, which under favorable conditions is estimated to be no larger than ± 10–15%.

Figs. 5a–5c show representative C_d–E curves gathered for bromide electrolytes, (0.5M $NaClO_4$ + xM NaBr with $x = 0$ to 0.1M), using electropolished (fig. 5a), and roughened silver having RF values of 1.9 (fig. 5b) and 4.2 (fig.

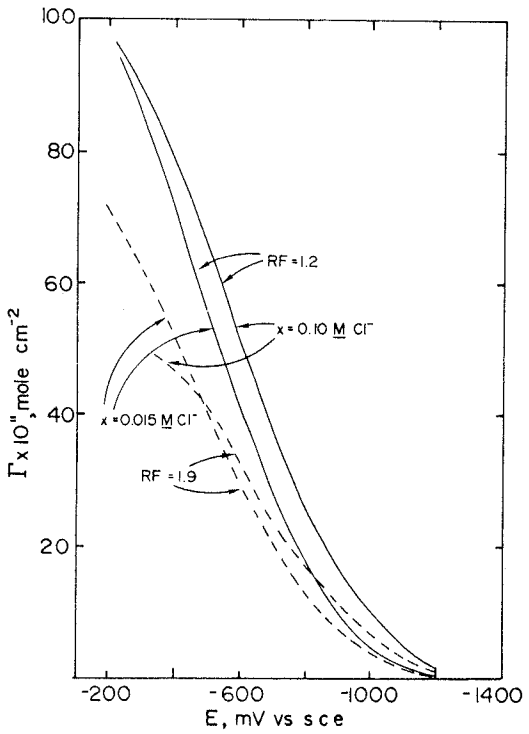

Fig. 4. Surface concentration of specifically adsorbed chloride (per cm^2 real area) at electropolished (solid curves) and roughened silver (dashed curves) versus electrode potential for bulk chloride concentrations of 0.015M and 0.10M, analyzed from figs. 3a and 3b as outlined in text.

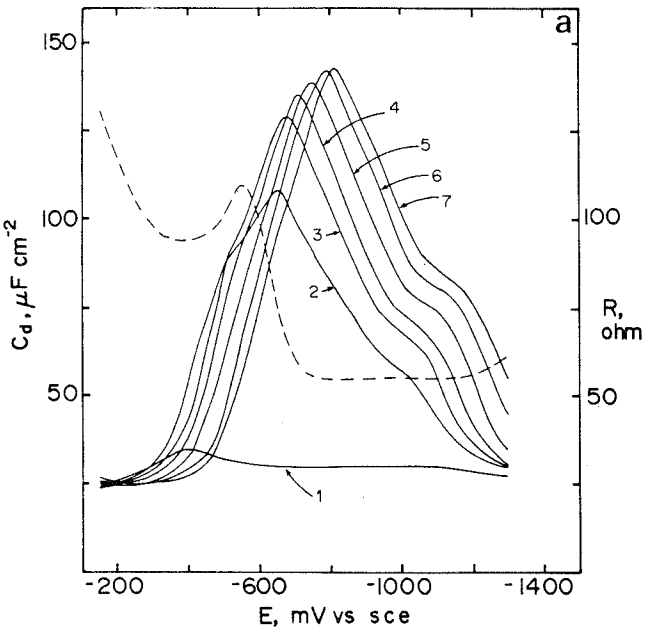
a
150
100
50
C_d, μF cm^{-2}
100
50
R, ohm
1
2
3
4
5
6
7
-200
-600
-1000
-1400
E, mV vs sce

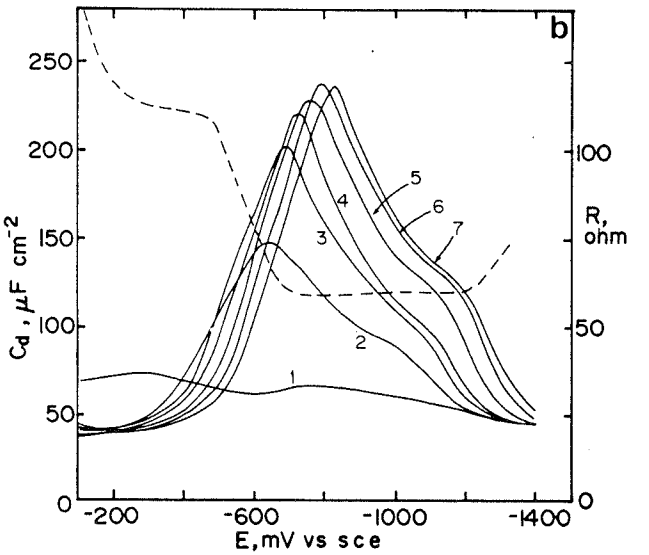
b
250
200
150
100
50
0
C_d, μF cm^{-2}
100
50
0
R, ohm
1
2
3
4
5
6
7
-200
-600
-1000
-1400
E, mV vs sce

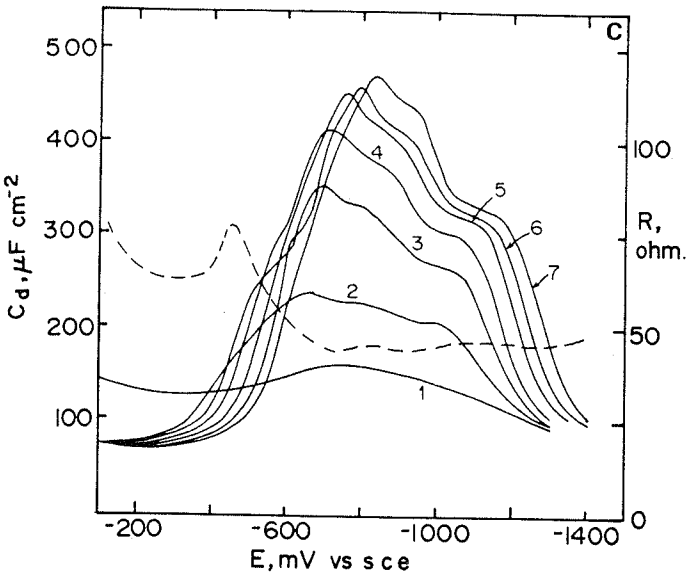

Fig. 5. (a) Differential capacitance versus electrode potential for electropolished polycrystalline silver in $NaClO_4$–NaBr mixtures of ionic strength 0.5. Key to bromide concentration (solid curves): (1) 0; (2) 0.6mM; (3) 2mM; (4) 5mM; (5) 15mM; (6) 40mM; (7) 100mM. The dashed curve is the cell resistance for 100mM bromide plotted on the same potential scale. (b) As (a), but for roughened silver (RF = 1.9). (c) As (a), but for roughened silver (RF = 4.2).

5c). Again, the shapes of the C_d–E curves on the roughened surfaces largely resemble those at the smooth electrode, the values of C_d being greater on the former to an extent that is approximately in accordance with the measured roughness factor. Fig. 6a shows the resulting plots of Γ'_{Br} against electrode potential for 0.015M bromide at these three surfaces, and fig. 6b shows the corresponding plot for 0.1M bromide. As for chloride, the values of Γ'_{Br} are marginally smaller on the roughened compared to the electropolished surface, and to an extent which increases with increasing roughness.

Figs. 5a–5c also show representative plots of the resistive component R of the measured impedance against potential for 0.1M bromide, shown as dashed curves. Although R is approximately constant beyond -700 mV, it exhibits sharp variations at potentials positive of the major C_d peak where high coverages of bromide are obtained. Similar behavior was observed for the other adsorbates studied here (cf. ref. [3]). Such variations are inconsistent with the usual representation of the interface as a pure "RC" circuit. The reason for this behavior is unclear, but may be associated with a sluggish restructuring of the adsorbate layer at high coverages. In any event, the derived Γ'_X values are clearly less trustworthy under these conditions.

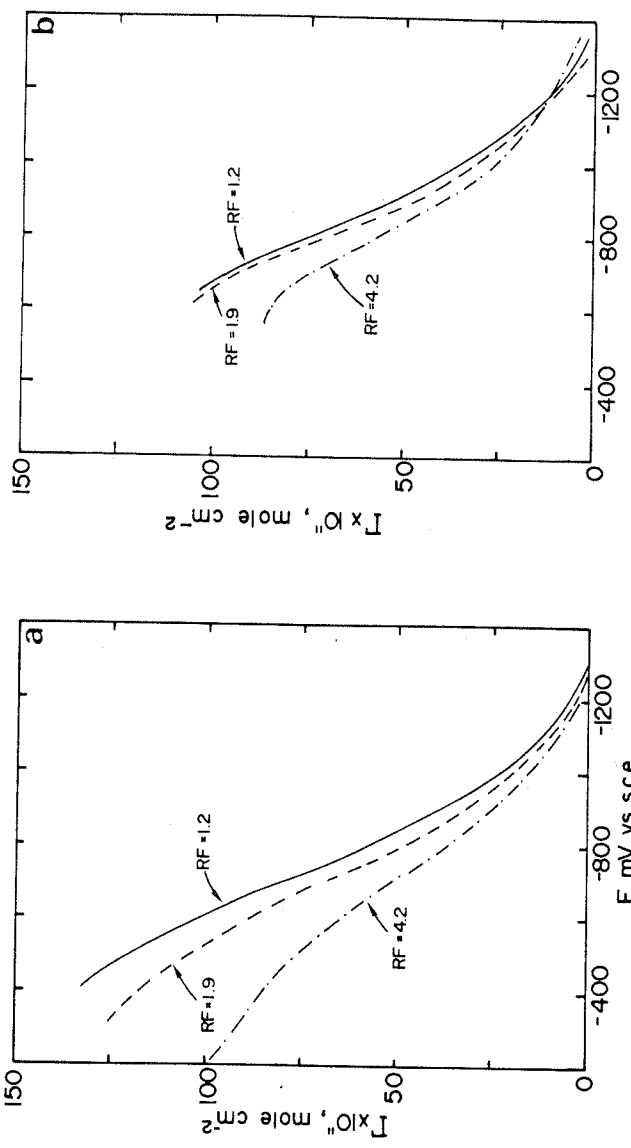

Fig. 6. (a) Surface concentration of specifically adsorbed bromide (per cm^2 real area) at electropolished (solid curve) and roughened silver (dashed, dotted-dashed curves) for bulk concentration x at 15mM obtained from figs. 5a and 5b. (b) As (a), but for $x = 100$mM.

Nevertheless, the shape of the C_d–E curves in the high coverage region can still yield useful information. The measured capacitance can be considered to consist of two components, one reflecting the dielectric properties of the particular interfacial composition ("constant coverage" capacitance) and an additional part arising from the variation in the adsorbate concentration with electrode potential [16]. This latter component will be greatest when the fractional surface coverage θ is about 0.5 because $(\partial\Gamma'_X/\partial E)_x$ and hence $(\partial q^m/\partial E)_x$ is anticipated to be a maximum at this point, and will vanish in the limits of low and saturation coverage since then $(\partial\Gamma'_X/\partial E)_x \to 0$. Therefore the major capacitance peak will occur at a surface coverage around 0.5, and the onset of concentration-independent and relatively potential-independent capacitances at more negative and positive potentials signal anion coverages that approach zero and unity, respectively. For chloride, the C_d–E curves converge only at positive potentials close to the onset of surface oxidation, ca. 0 mV. Bromide adsorption is sufficiently stronger so that the major capacitance peak occurs at more negative potentials and the C_d–E curves converge to a plateau at potentials positive of ca. −300 mV, indicating that a monolayer of adsorbed bromide is formed in this region. The surface concentration corresponding to a close-packed monolayer is estimated to be 1.6×10^{-9} and 1.35×10^{-9} mole cm^{-2} for chloride and bromide, respectively [3].

Figs. 7a and 7b show C_d–E curves for iodide-containing electrolytes obtained on electropolished and roughened electrodes, respectively, and figs. 8a and 8b show the same for thiocyanate. Both these anions are sufficiently strongly adsorbed to yield large increases in C_d upon their addition to 0.5M $NaClO_4$ even at the most negative potential (ca. −1300 mV) at which measurements could be made without interference from hydrogen evolution. This precludes a quantitative adsorption analysis since sizeable extrapolations to more negative potentials are required to a value where anion adsorption is negligible from which the C_d–E curves can be integrated. Nevertheless, once again the shapes of the C_d–E curves on the electropolished and roughened electrodes are similar, the latter merely exhibiting larger C_d values to an extent consistent with the roughness factor determined in 0.5M $NaClO_4$. Both iodide and thiocyanate are tenaciously adsorbed, apparently forming monolayers positive of ca. −900 mV for bulk anion concentrations of a few millimolar and above on the basis of the plateaus observed in the C_d–E curves under these conditions (figs. 7 and 8). However, the C_d–E curves for thiocyanate exhibit a pronounced structure in the more positive potential region, most notably yielding a large capacitance peak at ca. −250 mV which grows sharply as the bulk thiocyanate concentration is increased above 1 mM. The magnitude of this peak is noticeably dependent on the AC frequency, being markedly smaller at 1000 Hz than at 100 Hz; the latter was used to obtain the data in fig. 8. (No faradaic current was detected at these potentials.) In contrast, the C_d–E curves for iodide are featureless and essentially independent of the bulk iodide concentration in this region.

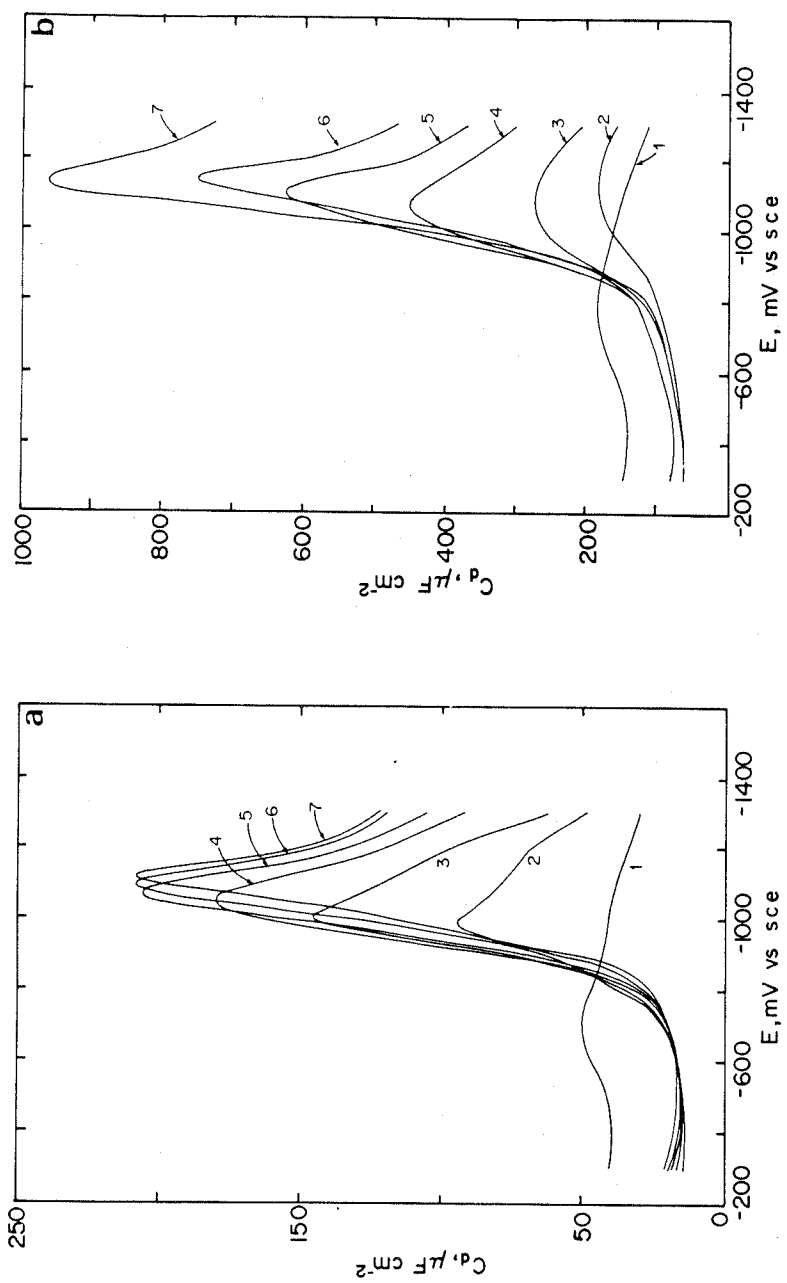

Fig. 7. (a) Differential capacitance versus electrode potential for electropolished silver in $NaClO_4$–NaI mixtures of ionic strength 0.5. Key to iodide concentrations: (1) 0; (2) 0.2mM; (3) 0.5mM; (4) 1.2mM; (5) 2.2mM; (6) 5mM; (7) 10mM. (b) As (a), but for roughened silver ($RF \approx 4.6$).

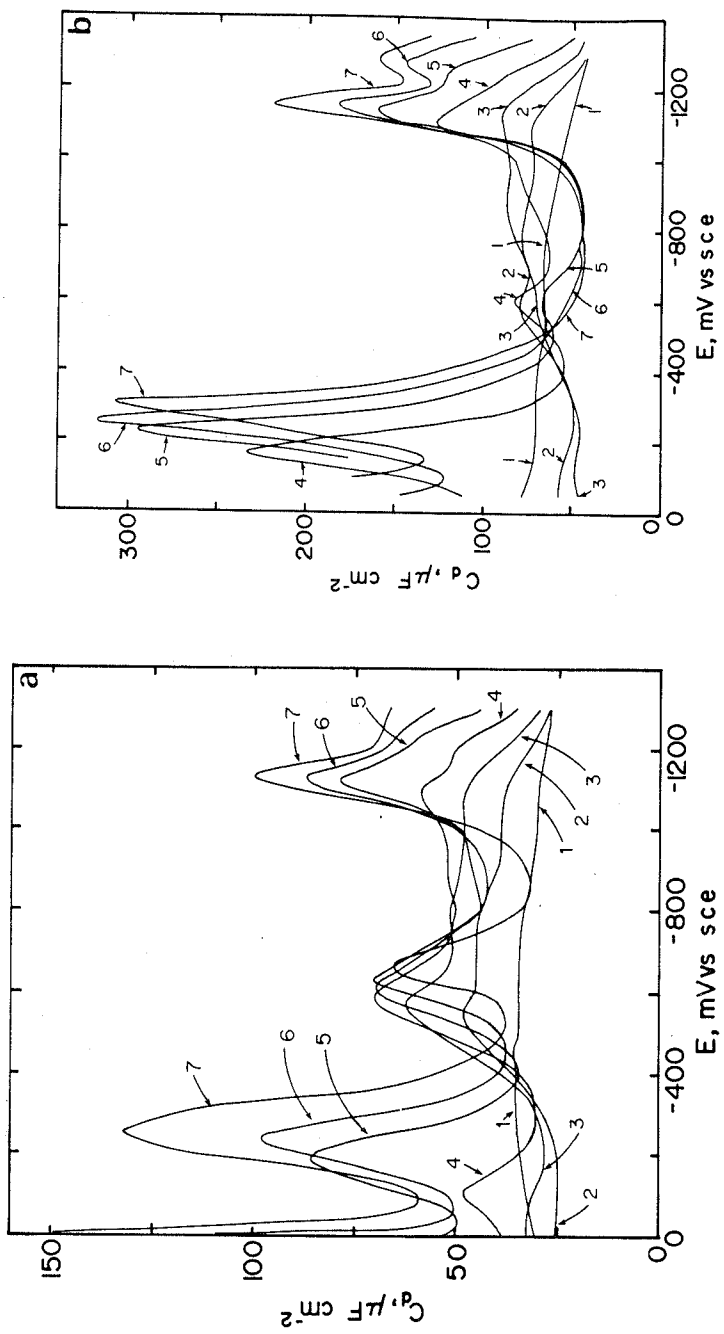

Fig. 8. (a) Differential capacitance versus electrode potential for electropolished silver in $NaClO_4$–NaNCS mixtures of ionic strength 0.5. Key to thiocyanate concentrations: (1) 0: (2) 0.3mM; (3) 1mM; (4) 3mM; (5) 10mM; (6) 30mM; (7) 100mM. (b) As (a), but for roughened silver (RF = 2.1).

It seems feasible that these additional features observed for thiocyanate are due to potential-dependent rearrangements of the adsorbate layer associated with alterations in the surface bonding geometry. Although thiocyanate very likely binds to metal surfaces preferentially via the sulfur atom [7], the nitrogen atom should also have some affinity for the silver surface which could result in a relatively flat or bent orientation. At more positive potentials, the enhanced electrostatic field at the silver surface resulting from larger positive electronic charge densities [2] and greater packing densities may increasingly favor a more perpendicular orientation with the NCS^- ion bound only via the sulfur where most of the anionic charge is located.

The corresponding C_d–E curves for azide at electropolished (fig. 9a) and roughened silver (fig. 9b) form an interesting comparison with the behavior of thiocyanate in view of the structural similarities of the two anions. Azide is sufficiently weakly adsorbed at the most negative potentials to allow values of Γ'_X to be determined. The resulting plots of Γ'_{N_3} versus E for azide concentrations of 0.01M and 0.1M at electropolished and roughened silver are shown in fig. 10. In contrast to chloride and bromide, azide yields significantly larger values of Γ'_X on the roughened compared to the electropolished surfaces. Although the extent of azide adsorption is comparable to that of bromide at relatively negative potentials, ca. -900 to -1200 mV, the increases in Γ'_{N_3} as the potential becomes less negative are less pronounced than those for bromide (fig. 6). Therefore values of Γ'_{N_3} close to that expected for a monolayer of azide adsorbed "end on", ca. 1.6×10^{-9} mole cm^{-2}, are barely attained even at the most positive potentials (ca. 0 mV), and at $x = 0.1$M (fig. 10). This feature can also be deduced from the shape of the C_d–E plots for azide (fig. 9); instead of the single major capacitance peak and a decrease to much smaller values at more positive potentials as seen for the halides, the azide curves exhibit two relatively shallow peaks. One possible reason for this more complicated behavior is that there is a change in orientation of the adsorbed azide with increasing coverage. A relatively flat orientation of the linear N_3^- ion which may be preferred at low coverages as a result of ligand–metal π overlap would need to give way to a more compact "end on" orientation in order to achieve surface concentrations above ca. 7×10^{-10} mole cm^{-2}.

Support for this interpretation is also obtained from the related observation that the "electrosorption valency" EV for azide depends markedly on the adsorbate coverage and electrode potential, changing from about 0.3 at the most negative potentials to about 0.15 in the potential region positive of the major C_d peak at ca. -900 mV. In contrast, adsorbed bromide exhibits values of EV close to 0.4 that do not decrease noticeably with potential or coverage until surface concentrations approaching saturation are reached. The former observation is nicely consistent with a change in azide orientation from flat to vertical in that this transformation would place the anionic charge further from the electrode. The vertical orientation would yield a smaller value of EV since

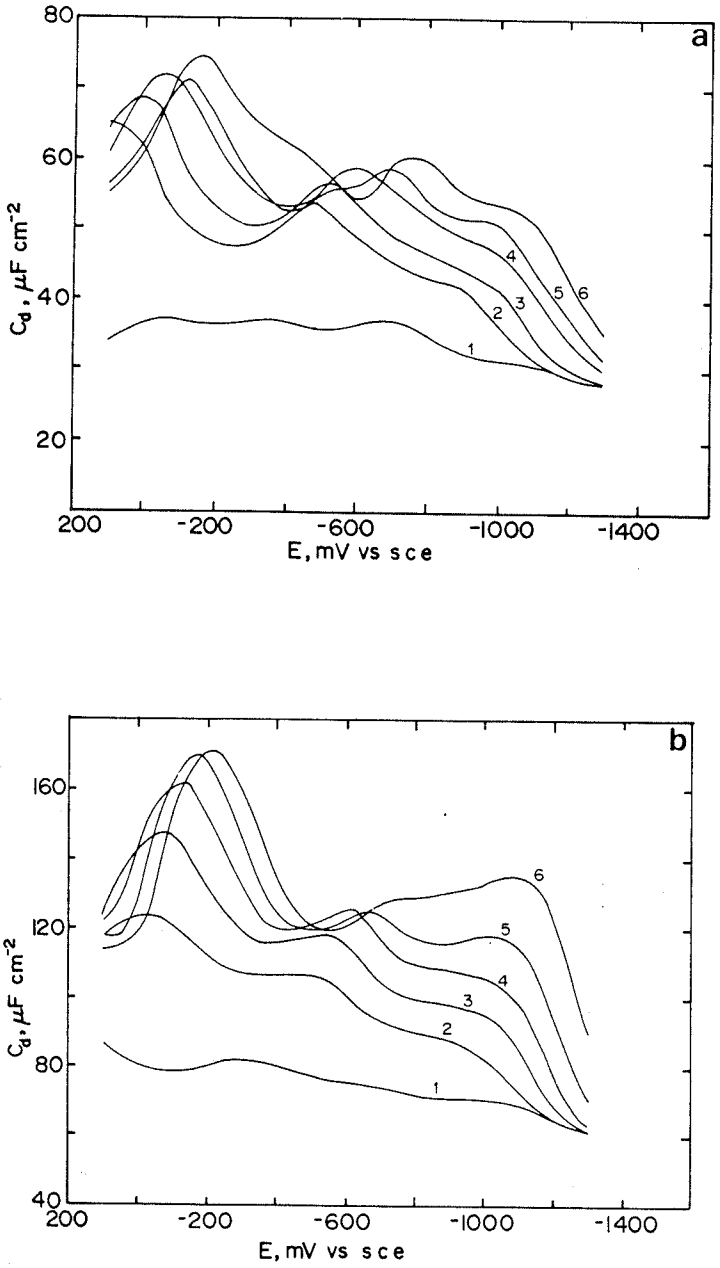

Fig. 9. (a) Differential capacitance versus electrode potential for electropolished silver in $NaClO_4$–NaN_3 mixtures of ionic strength 0.5. Key to azide concentrations: (1) 0; (2) 1mM; (3) 3mM; (4) 10mM; (5) 30 mM; (6) 100mM. (b) As (a), but for roughened silver (RF = 2.3).

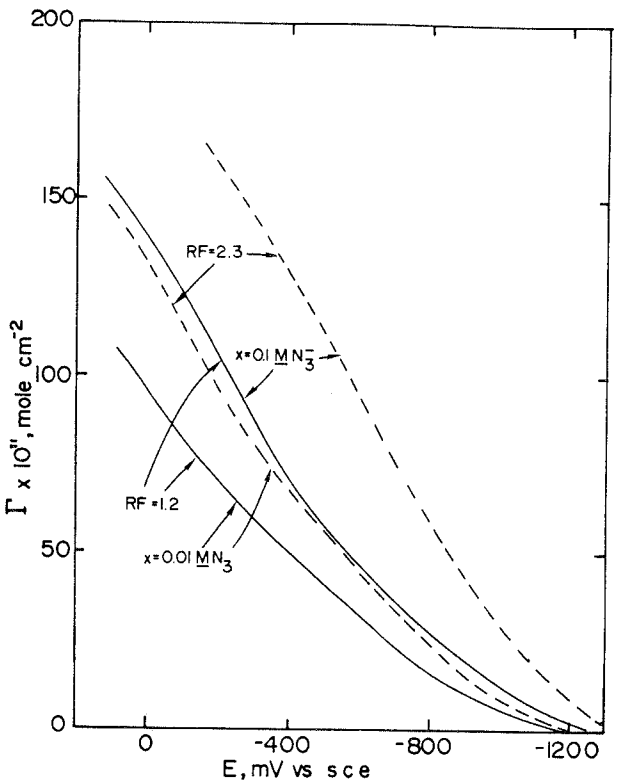

Fig. 10. Surface concentration of specifically adsorbed azide (per cm^2 real area) at electropolished (solid curves) and roughened silver (dashed curves) versus electrode potential for bulk azide concentrations of 0.01M and 0.1M, analyzed from figs. 9a and 9b as outlined in the text.

this quantity depends in part on the fraction of the double-layer potential drop traversed by the anionic charge upon adsorption [17,18].

Since the surface concentration data in figs. 4, 6, and 10 were obtained by using eq. (3), significant errors in Γ'_X may arise from perchlorate coadsorption [19]. Approximate estimates of their magnitude can be estimated by inspecting eq. (2) which takes this factor into account. In general eq. (3) will tend to underestimate Γ'_X since the second term in brackets in eq. (2), which is neglected in eq. (3), will always be positive. The error is most likely to be significant for the least strongly adsorbing anion, chloride, for which the largest bulk anion concentrations, and hence $x/(0.5 - x)$, are required in order to induce a given value of Γ'_X. Although Γ'_{ClO_4} is not known quantitatively, kinetic probe measurements indicate that in pure perchlorate media $F\Gamma'_{ClO_4} \sim q^m$ over a range of positive electrode charges [3,20,21], yielding $\Gamma'_{ClO_4} \sim 2.5$ to

3.5×10^{-10} mol cm^{-2} in the potential region ca. -200 to -400 mV. For high chloride concentrations, say $x = 0.1$ so that $x/(0.5 - x) = 0.25$, the apparent values of Γ'_X from eq. (3) are ca. 8 to 10×10^{-10} mol cm^{-2} in this potential region, so that the magnitude of the correction term $[x/(0.5 - x)]\Gamma'_{ClO_4}$, ca. 1×10^{-10} mol cm^{-2}, is small yet significant. However, the actual error in Γ'_X is almost undoubtedly smaller than this since strong chloride adsorption will inevitably diminish Γ'_{ClO_4} substantially. The errors in Γ'_X are likely to be negligible for smaller values of x and with the other adsorbing anions. Admittedly, the presence of adsorbed perchlorate may still influence the values of Γ'_X from eq. (3) but the analysis errors themselves appear to be minor.

Standard free energies for adsorption, ΔG_a°, were calculated for each anion at the effective potential of zero charge for polycrystalline silver, -930 mV, using the procedure outlined in ref. [3] with adsorbate and bulk standard states of 1 molecule cm^{-2} and 1 mole liter^{-1}, respectively. Typical values of ΔG_a° are: -95, -101 and -95 kJ mol^{-1} for chloride, bromide and azide at electropolished silver, and -92, -100 and -94 kJ mol^{-1} at roughened silver (RF $\approx$ 2). These values are somewhat more negative than those reported at polycrystalline silver in mixed 0.5M fluoride media [3]. This disparity is probably due in part to the diminution of anion adsorption in fluoride media caused by repulsive interactions with coadsorbed fluoride ions.

3.3. Surface crystallographic changes induced by electrochemical roughening

In addition to yielding quantitative information on the extent of specific ionic adsorption, the C_d–E curves can also provide useful clues to the crystallographic nature of the metal surface. Thus the shapes of the C_d–E curves obtained at single-crystal silver electrodes can be diagnostic of the particular crystallographic orientation exposed at the surface [2,5,8]. Moreover, a number of well-defined capacitance peaks are obtained in chloride and bromide electrolytes whose shape and potential are characteristic of the surface crystallographic orientation [2,8]. This suggests that comparison of C_d–E curves obtained for polycrystalline and various single-crystal surfaces in a given electrolyte could provide information on the crystallographic components of the former surface, and shed light on the structural changes induced by electrochemical roughening.

The major features of the C_d–E curves in, for example, 0.1M chloride at electropolished silver in fig. 3a are a shoulder at ca. -1000 mV (feature I) a major peak with a sharp summit at -550 mV (II), and a sharp peak at -100 mV (III). Upon roughening the electrode (fig. 3b), features I and II become more pronounced, and III is diminished. A C_d–E curve with similar features to those in fig. 3b was also obtained by Fleischmann et al. for highly roughened silver (RF ~ 15) in 0.1M NaCl [8]. Comparison with the C_d–E curves obtained for comparable chloride concentrations at silver surfaces having (111), (100),

and (110) orientations [2,8] reveal that feature I closely resembles that found for (110) crystallites, feature II with (100), and feature III with (111) crystallites. Consequently, it appears that electrochemical roughening in chloride media results in an increase in the proportion of facets resembling (100) and (110), and a decrease in those resembling (111) crystallites.

The C_d–E curves for bromide electrolytes are consistent with this interpretation. The two main features at electropolished polycrystalline silver in 0.1M bromide (fig. 5a) are a shoulder at ca. −1150 mV (I) and a major broad peak at −800 mV (II). Roughening the electrode (figs. 5b and 5c) results in a little change in II but yields a significant increase in I. Comparison with corresponding single-crystal data [2] suggests that feature II is probably formed from a composite of closely overlapping peaks from several low-index faces, whereas I is predominantly associated with the (110) and (100) faces. These and possibly other higher index planes therefore seem to be more prevalent on the roughened surfaces. This finding seems reasonable since metal oxidation and rapid redeposition would be expected to produce a relatively "loose" and somewhat disordered surface, with a smaller proportion of the most densely packed (111) planes.

Nevertheless it should be noted that the overall changes, both in the morphology of the C_d–E curves themselves and in the surface anion concentration induced by even quite extensive surface roughening are surprisingly mild, the major effect being simply to enhance the effective surface area. Thus although the morphology of the surface at the ca. 1 μm level that is probed by scanning electron microscopy is strikingly altered by electrochemical roughening [22] it appears that such large-scale surface reconstruction gives rise to only relatively minor alterations in the average crystallographic structure as well as in the average double-layer composition.

3.4. Implications for surface-enhanced Raman scattering

The enormous increases in the intensity of SERS brought about by electrochemical roughening of the type and magnitude employed here [23] stand in sharp contrast to the relatively moderate (ca. 1.5- to 4-fold) increases in the actual surface area and the minor changes in the surface concentration of adsorbed anions. This implies that the role of surface roughness in promoting SERS is to greatly enhance the inelastic scattering efficiency of the adsorbate scattering centers, in harmony with commonly held views [1,23]. Nevertheless, it is of considerable interest to ascertain the functional relationships, if any, between the intensity and nature (frequency, bandshape) of the Raman scattering and the average surface concentration of the Raman-active adsorbate. Such relationships are explored in detail for halide and pseudohalide adsorbates elsewhere [7,13]. We shall confine our remarks here to observations of a more qualitative nature.

The adsorption data presented here show that substantial specific adsorption of a number of anions occurs even at strongly negative potentials. Thus in the range of adsorbate concentrations 0.01M–0.1M, bromide, iodide, and thiocyanate are adsorbed with coverages above half a monolayer at potentials positive of about −800, −1150, and −1100 mV, judging by the position of the major peaks in the C_d–E curves (figs. 5–8). Although stable SERS signals are observed for these anions at potentials close to the anodic limit, ca. 0 to −250 mV, the scattering intensity is found to diminish to small or even imperceptible levels upon shifting the potential to these more negative values [7,24–26]. Moreover, as noted above for chloride, scanning the potential to such negative values and returning yields negligible hysteresis in the C_d–E curves and hence the Γ'_X–E plots, yet the SERS signals are almost entirely irreversibly quenched upon the return scan [7,25–26]. Further, comparisons between the present adsorption data and SERS spectra obtained under comparable conditions as a function of electrode potential for chloride, bromide, iodide [24], thiocyanate [7,25], and azide [26] indicate that in each case the Raman signals at a roughened silver electrode undergo rapid and irreversible decay as the potential is shifted negative only to the point where the anion coverage starts to fall below a monolayer. This point is signaled by an increase in C_d towards the major C_d–E peak. This result holds for Raman signals associated with both metal surface-ligand and internal vibrational modes. From figs. 3b, 5b, 5c, 7b, 8b and 9b, these potentials for $x \sim 0.01$M are ca. −200, −500, −900, −900, and +100 mV for chloride, bromide, iodide, thiocyanate, and azide, respectively. For azide, a monolayer is only formed close to the onset of metal dissolution at ca. 150 mV; indeed stable SERS spectra for this anion are not seen at more negative potentials [26] even though extensive azide adsorption occurs as far negative as ca. −800 mV (fig. 10).

A likely explanation for this surprising behavior is that the most efficient Raman scattering occurs from specific surface sites associated with particular morphologies, probably small metal clusters which are metastable with respect to incorporation into the metal lattice [27]. At adsorbate coverages close to a monolayer, anions will bind to these sites giving rise to SERS and will also occupy the large majority of nearby metal lattice sites. Although not contributing to the observed Raman signal, the latter adsorbate can stabilize the Raman-active clusters by preventing their dissipation into the surrounding lattice. Altering the potential to sufficiently negative values so that a fraction of this adsorbate is desorbed will provide lattice positions into which the least stable clusters can rearrange, leading to an irreversible decrease in the Raman intensity. However, judging by the essentially reversible nature of the C_d–E curves, this rearrangement process appears to involve only a small fraction of the metal surface.

These considerations provoke the desirability of examining the potential dependence of SERS on time scales that are sufficiently short that the

irreversible decay of the Raman signal does not occur. Data gathered under such conditions, largely using a spectrograph-optical multichannel analyzer arrangement for rapid time resolution, are starting to appear [7,13,28]. Comparison of corresponding specific adsorption and SERS data gathered under these conditions shows that an approximate proportionality between the Raman intensity and Γ'_X does indeed exist for chloride and bromide [13]. However, thiocyanate exhibits somewhat different behavior inasmuch as marked (ca. 3-fold) decreases in Raman intensity for the C–N stretching mode (ν_{CN}) occur under reversible conditions when the potential is made more negative in the region ca. −150 to −750 mV [29] even though the thiocyanate coverage is maintained near a monolayer throughout [7]. This behavior may be associated with the potential dependence of thiocyanate orientation that was suggested above [7]. Thus a change in adsorbate surface bonding to a less perpendicular orientation as the potential is made more negative would be expected to yield a decrease in the Raman scattering efficiency of the ν_{CN} mode since the component of the polarization vector normal to the surface would thereby be diminished [30].

Finally, it should be noted that considerably (ca. 10-fold) more intense Raman scattering can be obtained for several adsorbed anions such as chloride, bromide, and thiocyanate if the electrode surface is illuminated by the laser beam during the ORC [31,32]. Nevertheless, preliminary measurements indicate that such laser illumination has only a small influence upon the C_d–E curves recorded in the presence of such anions, indicating that only minor changes in both the effective surface area and the anion surface concentrations occur under these conditions [33].

Although preliminary, the above observations point to the desirability of correlating the nature and intensity of SERS signals with the interfacial composition, both from the standpoint of understanding the nature of the SERS effect itself and its utilization as a microscopic probe of electrochemical surface structure. It will clearly be important to study structurally simple adsorbates having known surface concentrations and well-defined bonding geometries in order to unravel the importance of such basic factors as surface concentration, surface bonding and stereochemistry to SERS.

Acknowledgments

The computer program used for the double integration of the capacitance data was written by H.Y. Liu. This work is supported in part by the Air Force Office of Scientific Research and the Office of Naval Research. M.J.W gratefully acknowledges a fellowship from the Alfred P. Sloan Foundation.

References

[1] See, for example, R.P. Van Duyne, in: Chemical and Biochemical Applications of Lasers, Vol. 4, Ed. C.B. Moore (Academic Press, New York, 1979) ch. 5.
[2] G. Valette, A. Hamelin and R. Parsons, Z. Physik. Chem. (NF) 113 (1978) 71.
[3] D. Larkin, K.L. Guyer, J.T. Hupp and M.J. Weaver, J. Electroanal. Chem. 138 (1982) 401.
[4] (a) H.D. Hurwitz, J. Electroanal. Chem. 10 (1965) 35;
(b) E. Dutkiewicz and R. Parsons, J. Electroanal. Chem. 11 (1966) 100.
[5] G. Valette and A. Hamelin, J. Electroanal. Chem. 45 (1973) 301.
[6] See, for example, B. Pettinger and H. Wetzel, Ber. Bunsenges. Physik. Chem. 85 (1981) 473.
[7] M.J. Weaver, F. Barz, J.G. Gordon II and M.R. Philpott, Surface Sci., 125 (1983) 409.
[8] M. Fleischmann, J. Robinson and R. Waser, J. Electroanal. Chem. 117 (1981) 257.
[9] G. Valette, J. Electroanal. Chem. 122 (1981) 285.
[10] A. Bewick and B. Thomas, J. Electroanal. Chem. 84 (1977) 127.
[11] A. Vashkyalis and O. Demontaite, Soviet Electrochem. 14 (1978) 1050.
[12] J.T. Hupp, D. Larkin, H.Y. Liu and M.J. Weaver, J. Electroanal. Chem. 131 (1982) 299.
[13] M.J. Weaver, J.T. Hupp, F. Barz, J.G. Gordon II and M.R. Philpott, to be published.
[14] M.J. Weaver and F.C. Anson, J. Electroanal. Chem. 65 (1975) 737.
[15] Analogous methods to I and II, but involving analysis carried out at constant q^m rather than E have been commonly utilized to determine specific ionic adsorption at mercury electrodes [4]. However, the present potential-based methods are more convenient for solid electrodes since only the electrode potential and not the charge can be measured accurately at such surfaces.
[16] P. Delahay, Double Layer and Electrode Kinetics (Interscience, New York, 1965) p. 103.
[17] J.W. Schultze and K.J. Vetter, J. Electroanal. Chem. 44 (1973) 63.
[18] M.J. Weaver and F.C. Anson, J. Electroanal. Chem. 58 (1975) 95.
[19] B.B. Damaskin, Soviet Electrochem. 7 (1971) 776.
[20] K.L. Guyer, S.W. Barr and M.J. Weaver, in: Proc. 3rd Symp. on Electrode Processes, Eds. S. Bruckenstein, J.D.E. McIntyre and B. Miller (Electrochem. Soc., Princeton, NJ, 1980) p. 390.
[21] S.W. Barr, K.L. Guyer and M.J. Weaver, J. Electroanal. Chem. 111 (1980) 41.
[22] J.F. Evans, M.G. Albrecht, D.M. Ullevig and R.M. Hexter, J. Electroanal. Chem. 106 (1980) 209.
[23] S.G. Schultz, M. Janick-Czachor and R.P. Van Duyne, Surface Sci. 104 (1981) 419.
[24] H. Wetzel, H. Gerischer and B. Pettinger, Chem. Phys. Letters 78 (1981) 392.
[25] H. Wetzel, H. Gerischer and B. Pettinger, Chem. Phys. Letters 80 (1981) 159.
[26] R.E. Kunz, J.G. Gordon II, M.R. Philpott and A. Girlando, J. Electroanal. Chem. 112 (1980) 391.
[27] W.J. Plieth, J. Phys. Chem. 86 (1982) 3166.
[28] J.F. Owen, T.T. Chen, R.K. Chang and B.L. Laube, paper presented at the Intern. Conf. on Electronic and Molecular Structure of Electrode–Electrolyte Interfaces, Logan, UT, 1982; Surface Sci., submitted.
[29] Note that the electrode potentials in ref. [7] are quoted versus Ag/AgCl (saturated KCl) which has a potential of about −45 mV on the SCE scale employed here.
[30] C.S. Allen and R.P. Van Duyne, Chem. Phys. Letters 63 (1979) 455;
G.C. Schatz and R.P. Van Duyne, Surface Sci. 101 (1980) 425.
[31] F. Barz, J.G. Gordon II, M.R. Philpott and M.J. Weaver, Chem. Phys. Letters, 91 (1982) 291.
[32] S.H. Macomber, T.E. Furtak and T.M. Devine, Chem. Phys. Letters, 90 (1982) 439.
[33] S. Farquharson, J.T. Hupp and M.J. Weaver, unpublished observations.